MOLECULAR AND CELLULAR BIOLOGY, Oct. 1999, p. 6929–6939 Vol. 19, No. 10
0270-7306/99/$04.00+0

The Morphogenesis Checkpoint in *Saccharomyces cerevisiae*: Cell Cycle Control of Swe1p Degradation by Hsl1p and Hsl7p

JOHN N. McMILLAN,[1] MARK S. LONGTINE,[2] REY A. L. SIA,[1] CHANDRA L. THEESFELD,[1] ELAINE S. G. BARDES,[1] JOHN R. PRINGLE,[2] AND DANIEL J. LEW[1]*

Department of Pharmacology and Cancer Biology, Duke University Medical Center, Durham, North Carolina 27710,[1] *and Biology Department, University of North Carolina, Chapel Hill, North Carolina 27599*[2]

Received 7 June 1999/Returned for modification 13 July 1999/Accepted 26 July 1999

In *Saccharomyces cerevisiae*, the Wee1 family kinase Swe1p is normally stable during G_1 and S phases but is unstable during G_2 and M phases due to ubiquitination and subsequent degradation. However, perturbations of the actin cytoskeleton lead to a stabilization and accumulation of Swe1p. This response constitutes part of a morphogenesis checkpoint that couples cell cycle progression to proper bud formation, but the basis for the regulation of Swe1p degradation by the morphogenesis checkpoint remains unknown. Previous studies have identified a protein kinase, Hsl1p, and a phylogenetically conserved protein of unknown function, Hsl7p, as putative negative regulators of Swe1p. We report here that Hsl1p and Hsl7p act in concert to target Swe1p for degradation. Both proteins are required for Swe1p degradation during the unperturbed cell cycle, and excess Hsl1p accelerates Swe1p degradation in the G_2-M phase. Hsl1p accumulates periodically during the cell cycle and promotes the periodic phosphorylation of Hsl7p. Hsl7p can be detected in a complex with Swe1p in cell lysates, and the overexpression of Hsl7p or Hsl1p produces an effective override of the G_2 arrest imposed by the morphogenesis checkpoint. These findings suggest that Hsl1p and Hsl7p interact directly with Swe1p to promote its recognition by the ubiquitination complex, leading ultimately to its destruction.

Entry into mitosis is triggered by the activation of Cdc2-type cyclin-dependent kinases (Cdc28p in *Saccharomyces cerevisiae*) by mitotic B-type cyclins (35, 37). Cyclin B-Cdc2 complexes can accumulate in an inactive form if the Cdc2 subunit is phosphorylated on a critical tyrosine residue (amino acid 19 in Cdc28p) and, in some cells, also on the adjacent threonine residue (10, 35). Checkpoint controls that regulate entry into mitosis utilize this inhibitory phosphorylation to restrain activation of Cdc2 until key cell cycle events have been completed (38, 42). Cdc2 tyrosine phosphorylation is catalyzed by Wee1-related kinases (Swe1p in *S. cerevisiae*), and dephosphorylation is catalyzed by Cdc25-related phosphatases (Mih1p in *S. cerevisiae*) (7, 10, 45). It is therefore of great interest to elucidate the regulatory pathways that control the activity of the Wee1 family and Cdc25 family enzymes.

In *S. cerevisiae*, Cdc28p Tyr19 phosphorylation is induced by the morphogenesis checkpoint, which helps to coordinate the nuclear cycle with the process of bud development (22, 33). For example, several environmental insults, including rapid changes in ambient temperature or osmolarity, trigger a temporary disruption of actin polarity, causing delays in bud formation. The morphogenesis checkpoint responds by delaying mitosis so that cells do not undergo nuclear division before a bud has been constructed, thus preventing the formation of binucleate cells (22, 33). The cell cycle delay induced by the morphogenesis checkpoint requires Swe1p (49). Swe1p abundance varies during the cell cycle as a result of regulated transcription and degradation. *SWE1* transcription is periodic, with a peak in late G_1 (24, 29, 49) phase, and Swe1p is stable early in the cell cycle but becomes unstable during G_2 and M phases as a consequence of Cdc28p activation by the B-type cyclins Clb1p to Clb4p (48). Thus, Swe1p accumulates during late G_1 and S phases and is degraded during G_2-M in the unperturbed cell cycle. However, Swe1p is stabilized in response to perturbations of actin organization, and the resulting persistence or continued accumulation of the protein (possibly in conjunction with changes in its activity and/or localization) leads to G_2 arrest (48).

Two putative upstream regulators of Swe1p, Hsl1p and Hsl7p, were discovered serendipitously during a genetic screen for mutations displaying synthetic lethality with a deletion of the amino terminus of histone H3 (*HSL* [histone synthetic lethal]) (29). Although the basis for the genetic interaction with histones was not clarified, the data suggested that Hsl1p and Hsl7p act in some manner to lower the level of Swe1p activity. In particular, it was found that *hsl1* and *hsl7* mutants displayed a G_2 delay that was eliminated upon deletion of *SWE1* (29). However, many mutants with defects in cell morphogenesis display similar Swe1p-dependent G_2 delays, produced by the morphogenesis checkpoint in response to the mutant defect (33). It is therefore important to determine whether Hsl1p and Hsl7p indeed act directly on Swe1p or whether they simply cause a morphogenesis defect that activates the checkpoint response.

The sequence of Hsl7p has not yet suggested possible biochemical activities for this protein, but homology searches have identified close relatives in several other eukaryotes, including *Schizosaccharomyces pombe* and humans (16, 29). In contrast, support for the hypothesis that Hsl1p is a direct negative regulator of Swe1p has come from the similarity between the kinase domain of Hsl1p and that of Nim1, an *S. pombe* protein that has been shown to directly phosphorylate and inhibit Wee1 (9, 40, 55). In addition, *HSL1* (also called *NIK1*) was isolated independently in a screen for *S. cerevisiae* genes that could serve as multicopy suppressors of a temperature-sensitive *cdc2* mutant in *S. pombe* (54). This circumstantial evidence suggests that Hsl1p may also act by directly phosphorylating and inhibiting Swe1p. Homology searches have revealed that *S. cerevisiae* contains two other kinases, Gin4p and Kcc4p, that

* Corresponding author. Mailing address: Department of Pharmacology and Cancer Biology, Box 3686, Duke University Medical Center, Durham, NC 27710. Phone: (919) 613-8627. Fax: (919) 613-8642. E-mail: daniel.lew@duke.edu.

TABLE 1. *S. cerevisiae* strains used in this study

Strain[a]	Relevant genotype
JMY1469	**a** *SWE1myc:HIS2*
JMY1503	**a** *SWE1myc:HIS2 hsl1ΔURA3*
JMY1505	**a** *SWE1myc:HIS2 hsl7ΔURA3*
JMY1507	**a** *SWE1myc:HIS2 hsl1ΔURA3 hsl7ΔURA3*
JMY1470	**a** *SWE1myc:HIS2 SWE1myc:TRP1*
JMY1477	**a** *SWE1myc:HIS2 SWE1myc:TRP1 hsl1ΔURA3*
JMY1475	**a** *SWE1myc:HIS2 SWE1myc:TRP1 hsl7ΔURA3*
JMY1479	**a** *SWE1myc:HIS2 SWE1myc:TRP1 hsl1ΔURA3 hsl7ΔURA3*
JMY1569	**a**/α *swe1ΔLEU2/SWE1 mih1ΔLEU2/MIH1 hsl1ΔURA3/HSL1*
JMY1570	**a**/α *swe1ΔLEU2/SWE1 mih1ΔLEU2/MIH1 hsl7ΔURA3/HSL7*
JMY1571	**a**/α *mih1ΔTRP1/MIH1 hsl1ΔURA3/HSL1 GAL:HSL7:LEU2/HSL7*
JMY1572	**a**/α *mih1ΔTRP1/MIH1 hsl7ΔURA3/HSL7 GAL:HSL1:LEU2/HSL1*
DLY657	**a** *cdc24-1 bar1*
DLY690	**a** *cdc24-1 swe1ΔLEU2 bar1*
JMY1284	**a** *GAL:HSL7:LEU2 cdc24-1 bar1*
JMY1495	**a** *GAL:HSL1:LEU2:HSL1:TRP1 cdc24-1 bar1*
JMY1472	**a** *SWE1myc:HIS2 cdc24-1 bar1*
JMY1494	**a** *SWE1myc:HIS2 SWE1myc:TRP1 cdc24-1 bar1*
JMY1493	**a** *SWE1myc:HIS2 SWE1myc:TRP1(3X) cdc24-1 bar1*
JMY1300	**a** *hsl1ΔURA3 cdc24-1 bar1*
JMY1301	**a** *hsl7ΔURA3 cdc24-1 bar1*
JMY1500	**a** *HSL1myc:URA3 bar1*
M-1295*	**a** *HSL7-3HA:kan*
M-1505*	**a** *GAL:SWE1myc:URA3*
M-1537*	**a** *GAL:SWE1myc:URA3 HSL7-3HA:kan*
JMY1521*	**a** *GAL:SWE1myc:URA3 HSL7-3HA:kan bar1ΔTRP1*
JMY1539*	**a** *GAL:SWE1myc:URA3 HSL7-3HA:kan hsl1ΔTRP1*
DLY1	**a** *bar1*
RSY342	**a** *GAL:SWE1myc:URA3 CDC28^{Y19F}:TRP1*
RSY361	**a** *GAL:SWE1myc:URA3 hsl1ΔURA3 CDC28^{Y19F}:TRP1 bar1*
RSY356	**a** *GAL:SWE1myc:URA3 hsl7ΔURA3 CDC28^{Y19F}:TRP1 bar1*
RSY366	**a** *GAL:SWE1myc:URA3 GAL:HSL1:LEU2 CDC28^{Y19F}:TRP1 bar1*
RSY370	**a** *GAL:SWE1myc:URA3 GAL:HSL7:LEU2 CDC28^{Y19F}:TRP1 bar1*

[a] *, strains in the YEF473A (6) background (*his3 leu2 trp1 ura3 lys2*). All other strains are in the BF264-15DU (43) background (*ade1 his2 leu2-3,112 trp1-1[a] ura3Δns*).

are approximately as similar to Nim1 as is Hsl1p (4, 25). Recently, it was suggested that these kinases play a redundant role in Swe1p regulation (4). However, none of these kinases has yet been shown to regulate Swe1p directly.

In this report, we provide evidence that both Hsl1p and Hsl7p are bona fide negative regulators of Swe1p that appear to function interdependently in a pathway that targets Swe1p for degradation. During a checkpoint response, Hsl1p and Hsl7p do not target Swe1p for degradation, suggesting that the checkpoint mechanism may stabilize Swe1p by inhibiting Hsl1p or Hsl7p function.

MATERIALS AND METHODS

Yeast strains and plasmids. Standard genetic and molecular biology methods (30, 46) were used to generate all strains and plasmids used in this study, except as indicated below. The yeast strains used are listed in Table 1. Plasmids containing the *swe1ΔLEU2* (7), *mih1ΔLEU2* (45), *GAL:SWE1myc:URA3* (33), *CDC28^{Y19F}:TRP1* (48), *hsl1ΔURA3* (29), and *hsl7ΔURA3* (29) alleles have been described previously; appropriate fragments were introduced into yeast strains by direct transformation and confirmed by diagnostic PCR (26) and phenotypic tests.

To create the *SWE1myc:HIS2* allele, a 2.6-kb *Eco*RI/*Bam*HI fragment containing the COOH terminus of *SWE1* tagged with one hemagglutinin (HA) epitope, 12 myc epitopes, and downstream sequences was isolated from pRS306-*GAL:SWE1myc* (33) and ligated into the *Eco*RI/*Bgl*II sites of vector YIpGAP2 (49). Digestion of this plasmid with *Kpn*I targets integration to the *SWE1* locus, creating a full-length *SWE1myc* allele tagged with *HIS2* adjacent to a 3′ truncated *SWE1*. To create the *SWE1myc:TRP1* allele, a 4.0-kb *Pst*I/*Bam*HI fragment containing the *SWE1* gene and flanking sequences was removed from plasmid pJM1024 (isolated from a YCp50 genomic library [44]) and ligated into the corresponding sites of vector YIplac204 (14). A 2.0-kb *Cla*I/*Bam*HI fragment from pRS306-*GAL:SWE1myc* (33) that carries the COOH terminus of *SWE1* tagged as described above was inserted in place of the corresponding untagged fragment in the YIplac204-*SWE1* plasmid to create a full-length *myc*-tagged *SWE1* expressed from the *SWE1* promoter. This plasmid was digested with *Eco*RV to target integration to the *TRP1* locus. In addition to transformants containing a single copy of the *SWE1myc:TRP1* allele, one transformant contained three copies integrated at *TRP1* as determined by Southern blot analysis. This allele is referred to as *SWE1myc:TRP1*(3X).

The *GAL:HSL1:LEU2* and *GAL:HSL7:LEU2* alleles were constructed by similar strategies. In each case, the 5′ end of the gene was amplified from genomic DNA by PCR. A *Bam*HI site was incorporated into each primer with the 5′ site just upstream of the start codon. The primers used were 5′-TTATTGGATCCACACGACATGACTGGTCAC-3′ and 5′-GTTTATTAGGATCCTCTAATGCTGCCATGCCG-3′ (*HSL1*) and 5′-GGTTCAGGATCCATATGCATAGCAACG-3′ and 5′-CATACGAAGGATCCCTGGTTCTTGGCAAAGC-3′ (*HSL7*). The PCR products (0.8 kb for *HSL1* and 0.7 kb for *HSL7*) were cut with *Bam*HI and ligated into the corresponding site of vector YIpG2 (13, 53), which placed the fragments downstream of the *GAL1* promoter. The YIpG2-*HSL1* plasmid was targeted to integrate at the *HSL1* locus by digestion with *Xba*I; this created a full-length *GAL:HSL1:LEU2* allele adjacent to a 3′ truncated *HSL1*. The YIpG2-*HSL7* plasmid was targeted to integrate at the *HSL7* locus by digestion with *Nru*I; this created a full-length *GAL:HSL7:LEU2* allele adjacent to a 3′ truncated *HSL7*. To create the *GAL:HSL1:LEU2:HSL1:TRP1* allele, a 7.3-kb *Bam*HI/*Sac*I fragment containing *HSL1* and surrounding genomic sequence was isolated from plasmid pNE30 (11) and ligated into the corresponding sites of the vector pRS304 (50). The resulting plasmid was digested with *Stu*I to target integration to the *GAL:HSL1:LEU2* locus, creating a strain that contains *GAL*-regulated *HSL1* adjacent to wild-type *HSL1* under its own promoter.

The *HSL7-3HA:kan* allele was constructed as described by Longtine et al. (27). To create the *HSL1myc:URA3* allele, a 0.65-kb fragment corresponding to the 3′ end of *HSL1* and including the last coding base of the *HSL1* open reading frame was amplified by PCR with primers (5′-CTCTAGAATCTAAAAAAGTAGGTGGGGG-3′ and 5′-CGTCGACTGAACGTCCGGCATTTCGAATTAC-3′) that placed an *Xba*I site upstream of the fragment and a *Sal*I site downstream. This PCR product was digested with *Xba*I and *Sal*I and inserted into *Xba*I/*Sal*I-digested pRS306-*GAL:SWE1myc* (33), thus replacing the entire *SWE1* open reading frame and upstream sequences with the COOH-terminal *HSL1* fragment. This created an in-frame fusion of the 3′ end of *HSL1* with the myc tag in the plasmid. The resulting plasmid was targeted to integrate at the *HSL1* locus by digestion with *Eco*RI, thus creating the *HSL1myc:URA3* allele adjacent to a 5′ deleted *HSL1*.

The *mih1ΔTRP1*, *bar1ΔTRP1*, and *hsl1ΔTRP1* alleles were constructed by using the PCR disruption method (5, 28) and plasmid pRS304 (50) as a template. The PCR products were transformed directly into yeast to delete all or nearly all of the open reading frames of interest. The PCR primers used were: 5′-TGGACAAACCAGGATTGAAGTCAGCGAGGGTGAAGAAACCGCGCGTTTCGGTGATGAC-3′ and 5′-AATAACGATCTTCTTGCGGGCCTGGGTAAATCTTCTCGGTTTTCCTGATGCGGTATTTTCTCCT-3′ for *MIH1*, 5′-CCATTACTGCTTTAACAAACGATGGCACTGGTCACTTAGAGCGCGTTTCGGTGATGAC-3′ and 5′-ACACTGCCCGAATTTGCCATAGTCGAGGATAATTCTAATTTAGTTTCCTGATGCGGTATTTTCTCCT-3′ for *BAR1*, and 5′-TCAAATAGGTTGGATATCCATCATACTACTTGCTACTAATGCGCGTTTCGGTGATGAC-3′ and 5′-GAATTTATGAACGTCCGGCATTTCGAATTACTCTCTCCACTTTCCTGATGCGGTATTTTCTCCT-3′ for *HSL1*. All disruptions were confirmed by diagnostic PCR (26).

Media, growth conditions, and cell synchrony. Strains were grown in YEPD (1% yeast extract, 2% Bacto Peptone, 2% dextrose, and 0.01% adenine), YEPS (YEPD but with 2% sucrose instead of dextrose), or YEPG (YEPD but with 2% galactose instead of dextrose) medium. For α-factor arrest-release experiments, exponentially growing cells (2×10^6 to 5×10^6 cells/ml) were incubated with 20 to 25 ng of α-factor (custom synthesized by Research Genetics, Huntsville, Ala.) per ml for 2 to 3 h, harvested by centrifugation, and resuspended in a fresh medium to release the α-factor-induced cell cycle block. *bar1* strains were used in all such experiments, and microscopic examination confirmed that >90% of the arrested cells were unbudded. Cells were arrested in G_2/M by incubation with 15 μg of nocodazole (Sigma, St. Louis, Mo.; stored as a 10-mg/ml stock solution in dimethylsulfoxide at −20°C) per ml for 3 to 4 h (18). Microscopic examination confirmed that >80% of the treated cells had large buds, indicative of G_2/M arrest.

Fluorescence staining and microscopy. To visualize nuclear DNA, cells were fixed in 70% ethanol for >1 h, harvested by centrifugation, and resuspended in 0.2 μg of DAPI (4′6-diamidino-2-phenylindole; Sigma). Cells were viewed on an Axioskop apparatus (Zeiss, Thornwood, N.Y.) equipped with epifluorescence and differential interference contrast optics. Images were captured by using a cooled model charge-coupled device (CCD) camera (Princeton Instruments, Princeton, N.J.). Microscopic images of whole yeast microcolonies were captured similarly.

Preparation of lysates, immunoprecipitation, immunoblotting, and phosphatase treatment. Yeast cells were washed with ice-cold H_2O and harvested by centrifugation. Cell pellets were stored frozen at −80°C. Lysates were made by resuspending the pellets in a lysis buffer containing 50 mM Tris-HCl (pH 7.5),

150 mM NaCl, 5 mM EDTA, 1% NP-40, 1 mM sodium pyrophosphate, 1 mM phenylmethylsulfonyl fluoride, 1 mM sodium orthovanadate, and 2 μg each of pepstatin A and leupeptin (Sigma) per ml and vortexing with acid-washed glass beads. Lysates were clarified by centrifugation for 8 min at 14,000 rpm in an Eppendorf Microfuge, and the protein concentration was determined by using the Bio-Rad (Hercules, Calif.) protein assay.

For electrophoresis and immunoblotting, 20 μg of total protein per gel lane were mixed with hot (95°C) 2× sample loading buffer (final concentrations, 62.5 mM Tris-HCl [pH 6.8], 1% sodium dodecyl sulfate [SDS], 25% glycerol, 355 mM β-mercaptoethanol, 0.01% bromophenol blue) and incubated at 95°C for 5 min prior to electrophoresis on SDS–6 or 8% polyacrylamide gels. Proteins were then transferred electrophoretically to nitrocellulose membranes (Schleicher and Schuell, Keene, N.H.) and stained with anti-myc (9E10; Santa Cruz Biotechnology, Santa Cruz, Calif.) or anti-HA (12CA5; Boehringer Mannheim, Indianapolis, Ind.) antibody. Before staining, membranes were blocked with 5% nonfat dry milk in phosphate-buffered saline (PBS) containing 0.1% Tween 20 (PBS-Tween). Primary antibodies were used at a 1:1,000 dilution in PBS-Tween containing 1% nonfat dry milk. The secondary antibody (horseradish peroxidase-conjugated goat anti-mouse immunoglobulin G; Jackson Immunoresearch Laboratories, West Grove, Pa.) was used at a 1:2,500 dilution in the same solution. Incubations were carried out for 1 h each and separated by three washes with PBS-Tween. Blots were developed with Renaissance Western Blot Chemiluminescence Reagent Plus (NEN Life Sciences Products, Boston, Mass.).

For immunoprecipitation, 200 μg of lysate was incubated for 1 h with 1 μl of antibody and then for a further 1 h with 30 μl of a 50% slurry of protein A-Sepharose (Sigma) at 4°C with gentle rocking. Beads were washed three times with lysis buffer (see above) without protease inhibitors and then heated in 1× sample loading buffer, and proteins were separated and immunoblotted as described above.

For phosphatase treatment of Hsl7p-HA, anti-HA immunoprecipitate from 400 μg of lysate was washed twice with lysis buffer (see above) and twice with a solution containing 50 mM Tris-HCl (pH 7.5), 150 mM NaCl, 1 mM sodium pyrophosphate, 1% Triton X-100, 1% sodium deoxycholate, and 0.1% SDS and then divided into three equal aliquots. These aliquots were resuspended in 40 mM PIPES (piperazine-*N*,*N*′-bis[2-ethanesulfonic acid]) (pH 6.0) containing 1 mM dithiothreitol, 7.5 mM phenylmethylsufonyl fluoride, 37.5 μg of aprotinin (Sigma) per ml, and 25 μg each of benzamidine (Sigma), leupeptin, and pepstatin A per ml. Type II potato acid phosphatase (0.14 U) (Sigma) was added to two of the samples, and all samples were incubated at 30°C for 30 min. Sodium orthovanadate (10 mM) was added to inhibit phosphatase activity in one of the samples.

Pulse-chase analysis of Swe1p-myc stability. *GAL:SWE1myc:URA3* cells were grown in YEPS at 30°C and induced to express Swe1p-myc by the addition of 2% galactose for 10 min or 3 h. Cells were then harvested by centrifugation, resuspended at a density of 10^8 cells/ml in a labeling medium (6.7 g of yeast nitrogen base without methionine and cysteine [Bio 101, Vista, Calif.] per liter, 2% sucrose, and 2% galactose, plus 0.25 mCi of Trans^{35}S-Label [ICN Pharmaceuticals, Costa Mesa, Calif.] per ml [0.183 mM]) and incubated for a further 10 min to label newly synthesized proteins with [^{35}S]methionine and cysteine. Labeled cells were collected by filtration, washed with a prewarmed medium, and resuspended at a density of 3×10^7 cells/ml in fresh YEPD or YEPG supplemented with 3 mM methionine and 0.5% Casamino Acids to prevent further labeling. Incubation was continued, and aliquots of cells were diluted into ice-cold 10 mM NaN_3, harvested by centrifugation, washed with ice-cold 10 mM NaN_3, and frozen at −80°C. For some experiments, the protocol was modified as follows: α-factor (50-ng/ml final concentration) or nocodazole (15-μg/ml final concentration) was added 1 h prior to the addition of galactose, and subsequent incubations were performed in media containing the same concentration of α-factor or nocodazole.

For analysis, cell pellets were lysed as described above, and Swe1p-myc was immunoprecipitated by using anti-myc antibody (see above) from samples containing 3 μCi of radioactive label. Immunoprecipitates were washed three times with a lysis buffer, heated for 5 min in 1× sample loading buffer, and separated in SDS–8% polyacrylamide gels. Dried gels were exposed to a Molecular Dynamics (Sunnyvale, Calif.) storage phosphor screen for 24 to 48 h, scanned on a Molecular Dynamics model 445 SI PhosphorImager, and analyzed with ImageQuant, version 1.2 software.

RESULTS

Negative regulation of Swe1p in unperturbed cells by a pathway involving both Hsl1p and Hsl7p. Swe1p-mediated inhibition of Cdc28p leads to a G_2 delay during which bud growth continues primarily at the bud tip, resulting in a distinctive elongated-bud morphology (7, 23). The finding that *hsl1* and *hsl7* mutants exhibited a *SWE1*-dependent elongated-bud phenotype originally suggested that Hsl1p and Hsl7p might be negative regulators of Swe1p (29). However, the mutant phenotypes are quite variable depending on the strain background and growth conditions (54; see below), raising the question of how generally this conclusion might apply. For example, in our strain background, the deletion of *HSL1* or *HSL7* did not cause a pronounced phenotype in cells growing exponentially on our standard medium (Fig. 1A, panels 1 to 3). However, when the populations approached the stationary phase, a fraction of the *hsl1*Δ and *hsl7*Δ cells displayed elongated buds; this effect was not seen if *SWE1* was also deleted (data not shown). In addition, doubling the copy number of *SWE1*, a manipulation that has little effect on otherwise wild-type cells (Fig. 1A, panel 5), caused a pronounced elongated-bud phenotype in *hsl1*Δ or *hsl7*Δ cells even during exponential growth (Fig. 1A, panels 6 and 7).

The phosphatase Mih1p antagonizes Swe1p activity by reversing the Swe1p-catalyzed phosphorylation of Cdc28p (45). In the course of other studies, we observed that the steady-state levels of Mih1p declined as populations approached the stationary phase (32), perhaps explaining why *hsl1*Δ or *hsl7*Δ strains would show a Swe1p-dependent G_2 delay only at high cell densities (see above). To investigate further the interplay among Swe1p, Mih1p, and Hsl1p-Hsl7p, we constructed double-mutant and triple-mutant strains. Although the deletion of *MIH1* (Fig. 1B, panel 5), like the deletion of *HSL1* or *HSL7* (Fig. 1B, panels 2 and 6), has little effect in otherwise wild-type cells, both *hsl1*Δ *mih1*Δ and *hsl7*Δ *mih1*Δ double mutants were inviable and produced extremely elongated buds, suggestive of G_2 arrest (Fig. 1B, panels 3 and 7). The deletion of *SWE1* restored normal growth to these strains (Fig. 1B, panels 4 and 8), confirming that the G_2 arrest was a result of Swe1p activity.

Taken together, these data suggest that Hsl1p and Hsl7p indeed function generally as negative regulators of Swe1p. This negative regulation appears to play a minor role in unperturbed cells unless the activity of Swe1p is artificially increased or the activity of Mih1p is decreased to the point that it cannot effectively antagonize the action of the unregulated Swe1p.

To ask if Hsl1p and Hsl7p function in the same or separate pathways for regulation of Swe1p, we constructed *hsl1*Δ *hsl7*Δ double-mutant strains. Like the *hsl1*Δ and *hsl7*Δ single mutants, a double mutant that was otherwise wild type showed no conspicuous abnormalities during exponential growth (Fig. 1A, panel 4). Upon approach to the stationary phase (data not shown) or when the *SWE1* copy number was doubled (Fig. 1A, panel 8), the double mutant displayed elongated buds, but this phenotype did not appear more severe than those of the single mutants. This panel of strains provides a very sensitive readout of Swe1p activity, because doubling the *SWE1* dose has a large effect. Thus, the absence of an additive or synergistic effect in the double mutant implies that it has no more active Swe1p than the single mutants, suggesting that Hsl1p and Hsl7p act in the same pathway to inhibit Swe1p.

We attempted to order the actions of Hsl1p and Hsl7p in this pathway by testing whether the overexpression of either gene could compensate for the loss of the other. However, no such rescue was observed (Fig. 1C), suggesting that neither Hsl1p nor Hsl7p can effectively down-regulate Swe1p on its own and hence that these proteins play interdependent roles in the same step of Swe1p control.

Function of Hsl1p and Hsl7p during the morphogenesis checkpoint response. If Hsl1p and Hsl7p really act directly as negative regulators of Swe1p, then excess Hsl1p or Hsl7p might cause an inappropriate inhibition of Swe1p that could override the G_2 delay imposed by the morphogenesis checkpoint. To test this possibility, we generated strains that expressed *HSL1* or *HSL7* under the control of the regulatable *GAL1* promoter and also harbored a temperature-sensitive *cdc24* mutation. At a restrictive temperature, the *cdc24* mutant

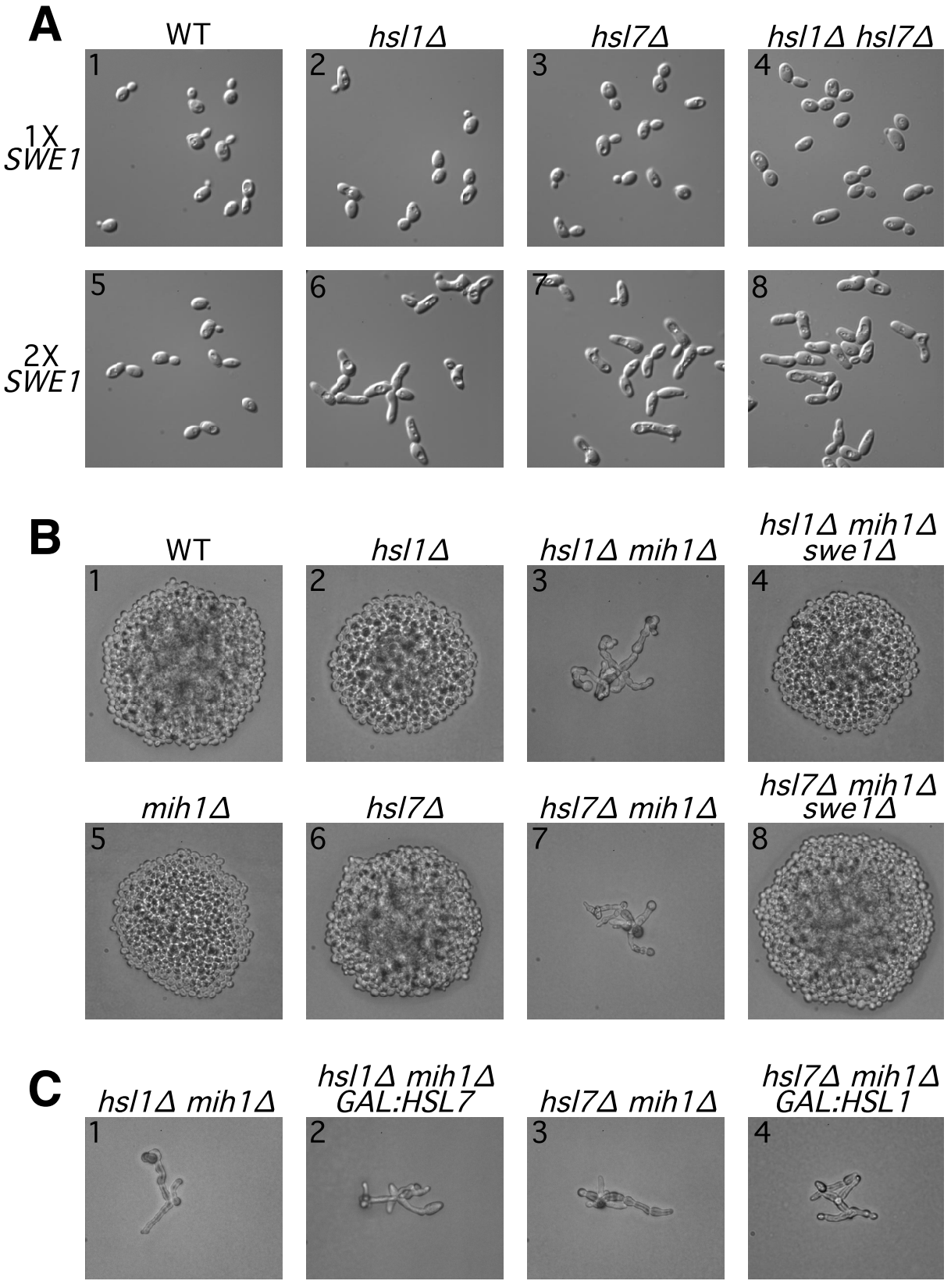

FIG. 1. Negative regulation of Swe1p in unperturbed cells by a pathway involving both Hsl1p and Hsl7p. (A) G_2 delay (resulting in bud elongation) when *SWE1* copy number is doubled in the absence of Hsl1p, Hsl7p, or both. Wild-type (WT) (JMY1469), *hsl1*Δ (JMY1503), *hsl7*Δ (JMY1505), and *hsl1*Δ *hsl7*Δ (JMY1507) strains and related strains containing an extra copy of *SWE1* (JMY1470, JMY1477, JMY1475, and JMY1479) were observed by using differential interference contrast optics during exponential growth (5×10^6 cells/ml) in YEPD medium. (B and C) Genetic interactions among *SWE1*, *HSL1*, *HSL7*, and *MIH1*. (B) Diploid strains JMY1569 (upper row) and JMY1570 (lower row) were sporulated to generate haploid segregants with the indicated genotypes (confirmed by replica plating and analysis of marker genes). Following tetrad dissection, spores were allowed to grow on YEPD medium for 2 days before the resulting microcolonies were photographed (C). Diploid strains JMY1571 (panels 1 and 2) and JMY1572 (panels 3 and 4) were sporulated, and spores of the indicated genotypes were grown on YEPG medium to induce overexpression of the *GAL*-regulated genes.

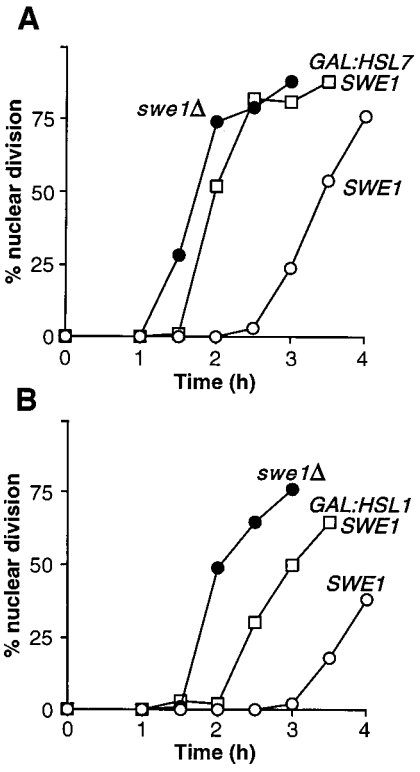

FIG. 2. Override of the morphogenesis checkpoint by overexpression of *HSL1* or *HSL7*. (A) Strains DLY657 (*cdc24-1 SWE1*) (○), DLY690 (*cdc24-1 swe1*Δ) (●), and JMY1284 (*cdc24-1 SWE1 GAL:HSL7:LEU2*) (□) were grown overnight at 24°C (permissive temperature) in YEPG to induce the *GAL* promoter, synchronized in G_1 phase with α-factor, and released into fresh YEPG at 37°C (restrictive temperature), where actin polarization and bud formation did not occur. At 30-min intervals, cells were fixed and stained to monitor the kinetics of nuclear division; 200 cells were scored in each sample. (B) Strains DLY657 (○), DLY690 (●), and JMY1495 (*cdc24-1 SWE1 GAL:HSL1:LEU2*) (□) were grown at 24°C in YEPS (noninducing nonrepressing medium for the *GAL* promoter) and arrested in G_1 phase with α-factor. Galactose was then added to induce the *GAL* promoter, and 1 h later the cells were released into fresh YEPG at 37°C and monitored as described above.

is unable to polarize actin and consequently exhibits a prolonged Swe1p-dependent G_2 delay (1, 22, 52) (Fig. 2A). However, when Hsl7p was overexpressed by growing the *GAL:HSL7* strain on galactose, the G_2 delay was virtually eliminated, and the cells traversed mitosis with kinetics similar to those of cells that lacked Swe1p altogether (Fig. 2A). The corresponding experiment for Hsl1p was more complicated because the constitutive overexpression of Hsl1p caused a Swe1p-independent growth defect associated with severe morphological aberrations (data not shown). However, when this problem was circumvented by growing the *GAL:HSL1* cells on galactose for only a short time, it was clear that the overexpression of Hsl1p could also override the checkpoint-induced G_2 delay of *cdc24* cells (Fig. 2B). It is not clear whether the less complete override of the checkpoint in this experiment reflects intrinsic differences in the abilities of Hsl1p and Hsl7p to inhibit Swe1p or simply a lesser degree of overexpression in the Hsl1p experiment. Nevertheless, these data suggest strongly that both Hsl1p and Hsl7p are bona fide negative regulators of Swe1p.

To investigate whether Hsl1p and Hsl7p normally play a role in the morphogenesis checkpoint response, we examined this response in cells with *HSL1* or *HSL7* deleted. Under the conditions used, the duration of the G_2 delay is very sensitive to *SWE1* gene dosage (49) (Fig. 3A). Nonetheless, the deletion of *HSL1* or *HSL7* did not produce a detectable lengthening of the G_2 delay in the *cdc24* mutant (Fig. 3B). The simplest interpretation of this result is that Hsl1p and Hsl7p are already turned off when the checkpoint response is induced, so that deleting the genes produces no additional increase in Swe1p activity (or, thus, in G_2 delay) under these conditions.

Periodic accumulation of Hsl1p during the cell cycle. To examine the behavior of Hsl1p and Hsl7p during the cell cycle, we generated strains expressing epitope-tagged versions of these proteins. The Hsl1p-myc and Hsl7p-HA proteins (expressed under the control of their own promoters at their normal genomic loci) were fully functional by the criteria that *HSL1myc:URA3 mih1ΔLEU2* and *HSL7-3HA:kan mih1ΔLEU2* strains were viable and had normal cell morphology (data not shown). In synchronized cells, Hsl1p-myc was absent in G_1, accumulated during S phase to a peak in G_2/M, and disappeared coincident with nuclear division (Fig. 4A). This pattern of protein accumulation is consistent with the previously described pattern of *HSL1* mRNA accumulation, which is periodic with a peak in late G_1 (54).

Periodic Hsl1p-dependent phosphorylation of Hsl7p. In contrast to Hsl1p, Hsl7p was present at approximately constant levels throughout the cell cycle (Fig. 4B). However, a fraction of the Hsl7p protein was modified in a cell cycle-dependent manner, as indicated by the periodic appearance of a more slowly migrating species (Fig. 4B). This species was also ap-

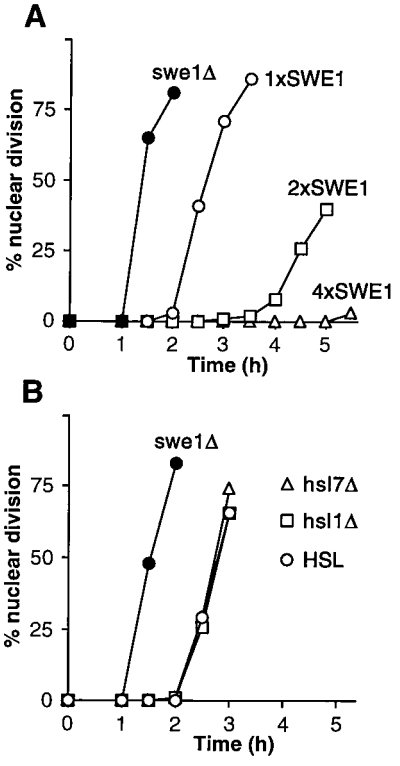

FIG. 3. Equivalent checkpoint delays in Hsl^+ and Hsl^- cells. (A) Strains JMY1472 (*cdc24-1 SWE1*) (○), DLY690 (*cdc24-1 swe1*Δ) (●), JMY1494 (*cdc24-1 2xSWE1*) (□), and JMY1493 (*cdc24-1 4xSWE1*) (△) were grown at 24°C (permissive temperature), synchronized in G_1 phase with α-factor, and released at 37°C (restrictive temperature), where actin polarization and bud formation did not occur. At 30-min intervals, cells were fixed and stained to monitor the kinetics of nuclear division; 200 cells were scored in each sample. (B) Strains DLY657 (*cdc24-1 SWE1*) (○), DLY690 (●), JMY1300 (*cdc24-1 SWE1 hsl1*Δ) (□), and JMY1301 (*cdc24-1 SWE1 hsl7*Δ) (△) were synchronized and analyzed as described for panel A.

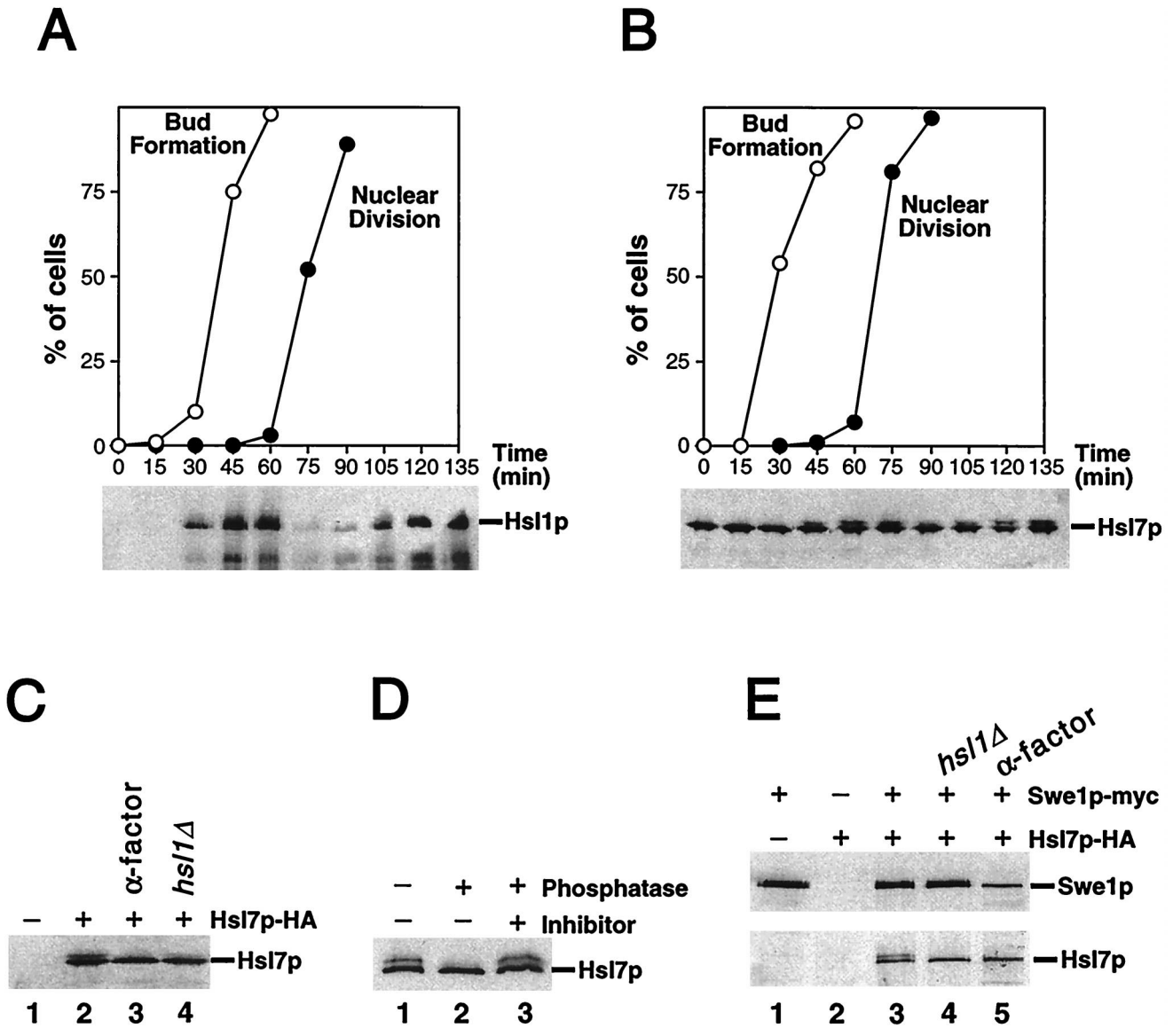

FIG. 4. Characterization of Hsl1p and Hsl7p. (A) Periodic accumulation of Hsl1p during the cell cycle. Wild-type cells expressing Hsl1p-myc (strain JMY1500) were grown in YEPD, synchronized in G_1 phase with α-factor, and released into a fresh medium. Cells were harvested at the indicated times, and separate aliquots were lysed to detect Hsl1p or fixed to monitor bud formation and nuclear division. Hsl1p-myc was immunoprecipitated from lysates containing 200 μg of total protein, separated by SDS-polyacrylamide gel electrophoresis (PAGE), and immunoblotted with anti-myc antibody. (B to D) Hsl1p-dependent phosphorylation of Hsl7p during the cell cycle. (B) Wild-type cells expressing Hsl7p-HA (strain JMY1521) were synchronized as described above. Lysates containing 20 μg of total protein were separated by SDS-PAGE, and Hsl7p-HA was detected by immunoblotting with anti-HA antibody. (C) Lysates were prepared from an Hsl7p-HA-expressing strain (JMY1521) that had been arrested in G_1 phase with α-factor (lane 3) and from cells of strains expressing or lacking Hsl7p-HA, Swe1p-myc (*GAL* regulated), and Hsl1p as indicated (lane 1, M-1505; lane 2, M-1537; and lane 4, JMY1539) that had been arrested in G_2 phase by growth for 3 h after galactose was added to induce overexpression of Swe1p-myc. Proteins were separated by SDS-PAGE and Hsl7p-HA was detected by immunoblotting with anti-HA antibody. (D) Anti-HA immunoprecipitates were prepared from lysate of a strain (M-1537) expressing Hsl7p-HA and divided into three equal aliquots that were subjected to a mock phosphatase treatment (lane 1), treatment with potato acid phosphatase (lane 2), or treatment with phosphatase together with the phosphatase inhibitor sodium orthovanadate (lane 3). Proteins were separated by SDS-PAGE, and Hsl7p-HA was detected by immunoblotting with anti-HA antibody. (E) Coimmunoprecipitation of Hsl7p-HA with Swe1p-myc. Lysates were prepared from strains expressing Hsl7p-HA, Swe1p-myc (*GAL* regulated), and/or Hsl1p, as indicated (lane 1, M-1505; lane 2, M-1295; lane 3, M-1537; and lane 4, JMY1539), that had been arrested in G_2 phase as described for panel C. Lysate was also prepared from a strain expressing both tagged proteins that had been arrested in G_1 phase with α-factor (JMY1521 [lane 5]). Anti-myc immunoprecipitates were prepared from samples containing 200 μg of total protein, separated by SDS-PAGE, and immunoblotted with anti-myc (upper blot) or anti-HA (lower blot) antibody.

parent in cells that had been arrested in G_2 by overexpression of Swe1p (Fig. 4C, lane 2), suggesting that Clb1p-4p–Cdc28p activity was not required for Hsl7p modification. Because the appearance of the modified Hsl7p protein was correlated with the peak in Hsl1p abundance during the cell cycle, we tested whether the modification was Hsl1p dependent. Indeed, the modified Hsl7p protein was not detectable in an *hsl1*Δ strain (Fig. 4C, lane 4). The modified Hsl7p protein disappeared following phosphatase treatment (Fig. 4D), indicating that the modification was phosphorylation. Thus, Hsl1p promotes the periodic phosphorylation of Hsl7p. It is not yet clear whether this effect is direct or indirect.

Hsl1p-independent association of Hsl7p with Swe1p. To determine if the negative regulation of Swe1p by Hsl7p reflects a

physical interaction, we tested for coimmunoprecipitation of these proteins. Indeed, when immunoprecipitates were prepared with anti-myc antibodies from cells expressing both Swe1p-myc and Hsl7p-HA, the latter protein was readily detected by immunoblotting (Fig. 4E, lane 3). In control experiments with cells expressing just one of the tagged proteins, no Hsl7p-HA was detected (Fig. 4E, lanes 1 and 2). Both phosphorylated and unphosphorylated forms of Hsl7p were coimmunoprecipitated with Swe1p (Fig. 4E, lane 3), and the association did not depend on Hsl1p (Fig. 4E, lane 4) and was detectable in cells arrested in G_1 by α-factor (Fig. 4E, lane 5). These data are consistent with the hypothesis that Hsl7p is a direct regulator of Swe1p.

Dependence of Swe1p degradation on Hsl1p and Hsl7p during the unperturbed cell cycle. Swe1p is normally stabilized in response to activation of the morphogenesis checkpoint (see the introduction). If the checkpoint acts (at least in part) by down-regulation of Hsl1p and/or Hsl7p, then the deletion of *HSL1* or *HSL7* should also result in Swe1p stabilization. Indeed, pulse-chase experiments (Fig. 5) showed that Swe1p was dramatically stabilized in both *hsl1*Δ and *hsl7*Δ strains, relative to the wild type, suggesting that Hsl1p and Hsl7p are required to target Swe1p for degradation.

Cell cycle-specific acceleration of Swe1p degradation by overexpression of Hsl1p. If Hsl1p or Hsl7p is rate limiting for Swe1p degradation, then the overexpression of one or both of these proteins might accelerate Swe1p degradation. To test this possibility, we performed pulse chase experiments in strains that simultaneously overexpressed Swe1p and Hsl1p or Swe1p and Hsl7p. It was observed previously that the overexpression of Swe1p in such experiments slows its degradation, presumably by saturating the capacity of a limiting component involved in Swe1p degradation (48) (also compare WT in Fig. 6 with WT in Fig. 5, in which Swe1p was not overexpressed). Strikingly, the overexpression of Hsl1p (but not of Hsl7p) accelerated Swe1p degradation (Fig. 6), suggesting that Hsl1p levels are rate limiting for Swe1p degradation, at least under conditions of overexpression.

Swe1p is normally stable during G_1 and unstable during G_2/M (48). Given the data described above, it seemed possible that the stability of Swe1p in G_1 cells might be due simply to the absence of Hsl1p. The acceleration of Swe1p degradation upon overproduction of Hsl1p (Fig. 6) might reflect either more efficient degradation during G_2/M, inappropriate degradation during G_1, or both. To distinguish among these possibilities, we repeated the experiment whose results are shown in Fig. 6 with cells synchronized in G_1 with α-factor or in G_2/M with nocodazole. As shown in Fig. 7A, Swe1p was stable in G_1 cells even when Hsl1p was overexpressed. In contrast, excess Hsl1p promoted more rapid Swe1p degradation in the G_2/M-arrested cells (Fig. 7B). Thus, Hsl1p appears to be rate limiting for degradation of overproduced Swe1p, but only at later stages of the cell cycle, suggesting the existence of a cell cycle-regulated step in Swe1p degradation in addition to the periodic accumulation of Hsl1p.

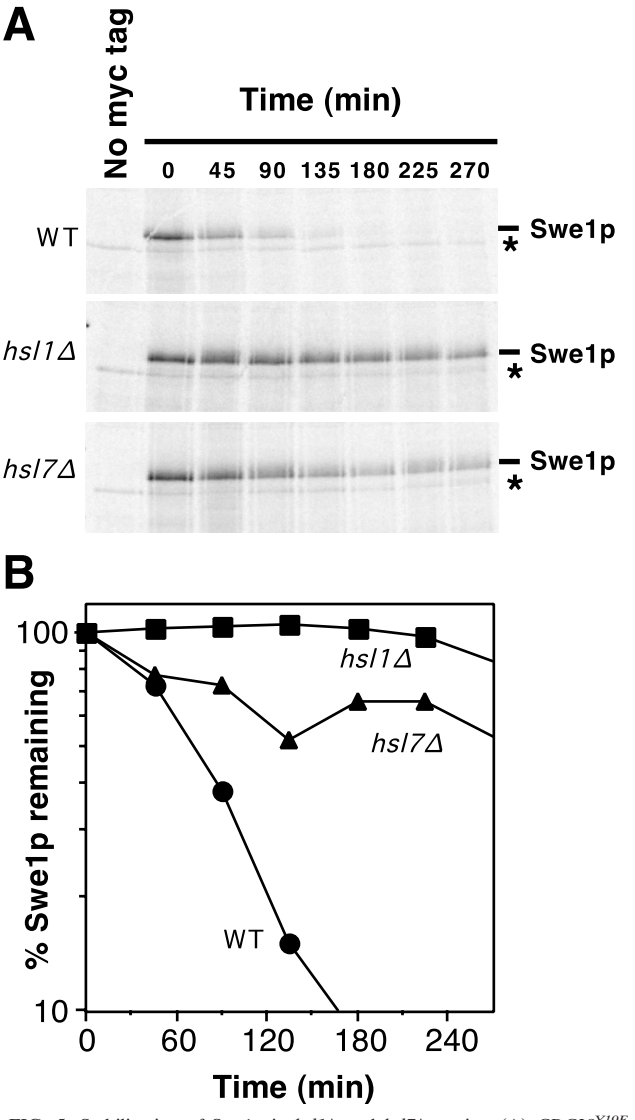

FIG. 5. Stabilization of Swe1p in *hsl1*Δ and *hsl7*Δ strains. (A) *CDC28*^{Y19F} *GAL:SWE1myc* strains RSY342 (wild type [WT]) (*HSL1 HSL7*) (top), RSY361 (*hsl1*Δ *HSL7*) (middle), and RSY356 (*HSL1 hsl7*Δ) (bottom) were grown in YEPS and induced to express Swe1p-myc by 10 min of growth in the presence of galactose. The cells were harvested, pulse labeled with [^{35}S]methionine and cysteine for 10 min, harvested again, and resuspended in fresh YEPD (to repress the *GAL* promoter) containing nonradioactive methionine and cysteine. The amounts of ^{35}S-labeled Swe1p-myc were determined at intervals by immunoprecipitation and SDS-PAGE. Cells of a strain (DLY1) not expressing Swe1p-myc were pulse labeled and processed as described above, providing a control shown in the left-hand lane of each gel. The asterisk indicates a labeled band that is present in cells lacking Swe1p-myc (left lanes) and binds to the protein A beads used for immunoprecipitation. (B) The radioactive signals from the gels shown in panel A were quantitated with a phosphorimager. These experiments were performed with *CDC28*^{Y19F} strains to avoid potential complications arising from the dependence of Swe1p degradation on Cdc28p activity (48); i.e., if the Swe1p produced during the pulse substantially inhibited Cdc28p, an artifactual stabilization of Swe1p might be observed during the chase period. However, Cdc28p^{Y19F}, which lacks the Swe1p phosphorylation site, is largely resistant to inhibition by Swe1p. We confirmed that cell proliferation indeed continued through the pulse-chase protocol in all strains (data not shown).

DISCUSSION

Down-regulation of Swe1p by Hsl1p and Hsl7p. It was observed previously that *hsl1* and *hsl7* mutants display a Swe1p-dependent G_2 delay, suggesting that Hsl1p and Hsl7p act as negative regulators of Swe1p (29). However, many mutants defective for aspects of cell morphogenesis also display Swe1p-dependent G_2 delays (22, 33), so that it was not clear whether Hsl1p and Hsl7p were involved primarily in morphogenesis or acted more directly on Swe1p. Our finding that the overexpression of Hsl1p or Hsl7p can override a morphogenesis checkpoint-induced G_2 delay provides a strong argument that these proteins function directly in down-regulating Swe1p. This down-regulation appears to depend, at least in part, on targeting Swe1p for degradation. The stability of Swe1p normally varies

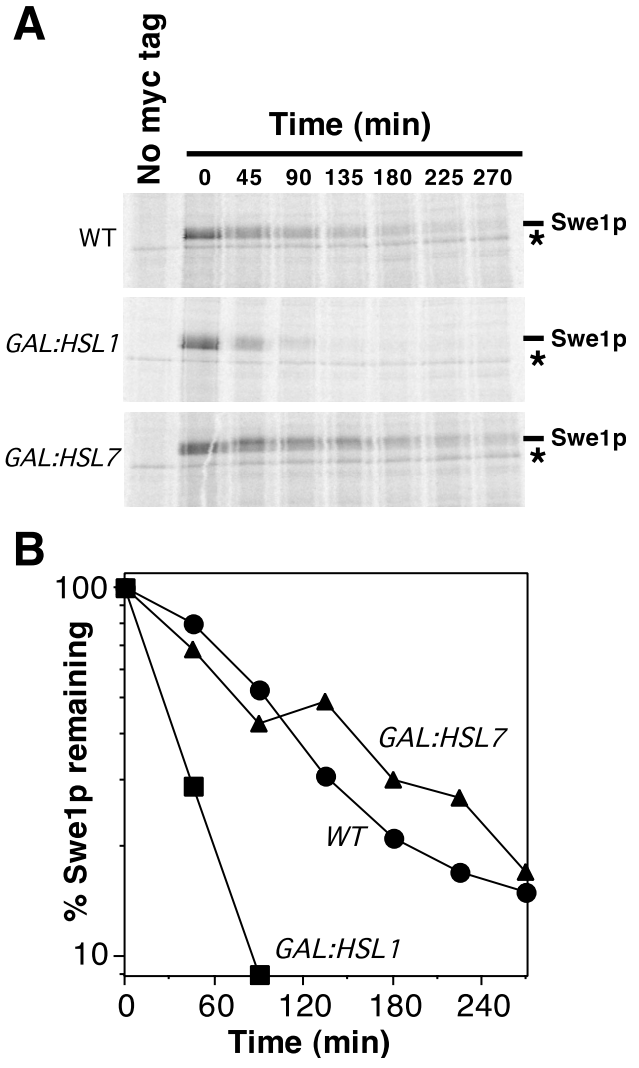

FIG. 6. Acceleration of Swe1p degradation by overexpression of Hsl1p. (A) *CDC28*^{Y19F} *GAL:SWE1myc* strains RSY342 (WT), RSY366 (*GAL:HSL1*), and RSY370 (*GAL:HSL7*) were grown in YEPS and induced to overexpress the *GAL*-regulated genes by addition of galactose for 3 h. The cells were harvested, pulse labeled with [^{35}S]methionine and cysteine for 10 min, harvested again, and resuspended in fresh YEPG containing nonradioactive methionine and cysteine. The amount of ^{35}S-labeled Swe1p-myc was determined by immunoprecipitation and SDS-PAGE. The asterisk indicates a labeled band that is present in cells lacking Swe1p-myc (left lanes) and binds to the protein A beads used for immunoprecipitation. (B) The radioactive signals from the gels shown in panel A were quantitated with a phosphorimager.

during the cell cycle: it is moderately stable during G_1 and becomes quite unstable in G_2/M (48). Our data indicate that both Hsl1p and Hsl7p are required for the rapid degradation of Swe1p and that Hsl1p is rate limiting for Swe1p degradation, at least under conditions of Swe1p overexpression. In addition, the genetic data indicate that Hsl1p and Hsl7p act in a single pathway to down-regulate Swe1p and that neither one can effectively down-regulate Swe1p in the absence of the other.

It has been shown previously that Swe1p degradation involves its ubiquitination by a complex, called SCF^{Met30}, that contains the F box protein Met30p and the ubiquitin-conjugating enzyme Cdc34p (19). Detailed analyses of the ubiquitination of the Cdc28p inhibitor Sic1p by a similar complex, SCF-^{Cdc4}, have revealed that phosphorylation of Sic1p is a necessary prelude to its ubiquitination and subsequent degradation (3, 12, 31, 51). Swe1p, like Sic1p, becomes hyperphosphorylated prior to its degradation (48). Thus, it is plausible that a part of this hyperphosphorylation is due to Hsl1p (in conjunction with Hsl7p) and that this phosphorylation targets Swe1p for recognition and ubiquitination by SCF^{Met30}. Swe1p degradation also requires Clb-Cdc28p activity (48). Our data indicate that Hsl1p overexpression accelerates Swe1p degradation during G_2/M but is unable to do so during G_1. Taken together, the data suggest that Clb-Cdc28p activity is required either to activate Hsl1p-Hsl7p or to collaborate with Hsl1p-Hsl7p in targeting Swe1p for degradation (Fig. 8A).

The conclusion that Hsl1p is a negative regulator of Swe1p was anticipated because the Hsl1p kinase domain (although not the large noncatalytic domain) is closely related to that of *S. pombe* Nim1, which is a negative regulator of Wee1. However, the finding that Hsl1p targets Swe1p for degradation was surprising, because Nim1 has been shown to phosphorylate Wee1 directly, inhibiting its kinase activity (9, 40, 55). We do

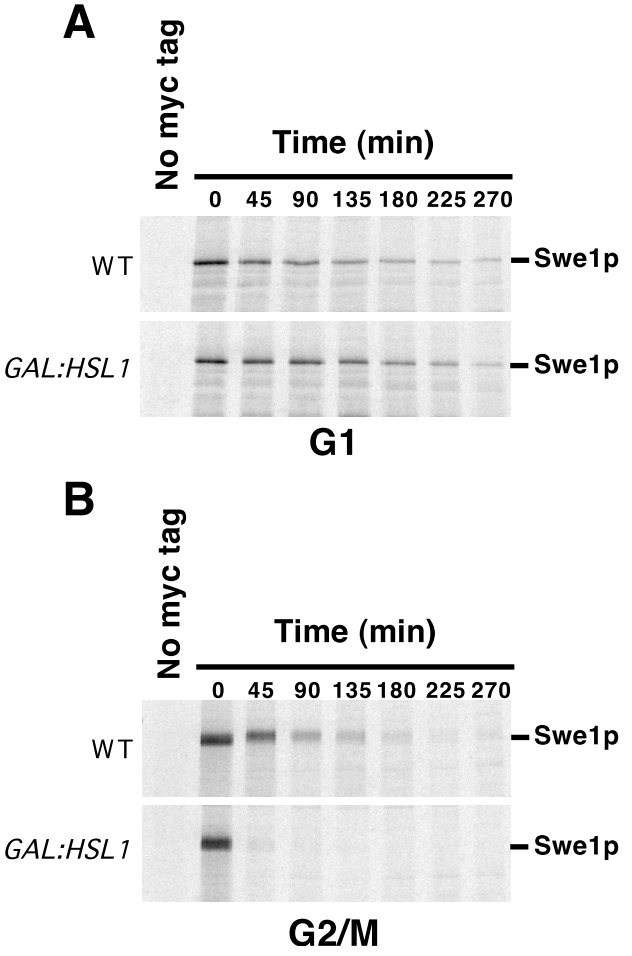

FIG. 7. Cell cycle specificity of the acceleration of Swe1p degradation by overexpression of Hsl1p. *CDC28*^{Y19F} *GAL:SWE1myc* strains RSY342 (WT) and RSY366 (*GAL:HSL1*) were grown in YEPS and induced to overexpress the *GAL*-regulated genes by addition of galactose. Just after galactose addition, the culture was split, and α-factor (50 ng/ml) was added to one set (A) while nocodazole (15 μg/ml) was added to the other (B). After incubation for 4 h, the cells were harvested, pulse labeled with [^{35}S]methionine and cysteine for 10 min, harvested again, and resuspended in fresh YEPG containing nonradioactive methionine and cysteine. The labeling and chase media also contained α-factor or nocodazole to maintain the cell cycle arrest throughout. The amount of ^{35}S-labeled Swe1p-myc remaining was determined by immunoprecipitation and SDS-PAGE.

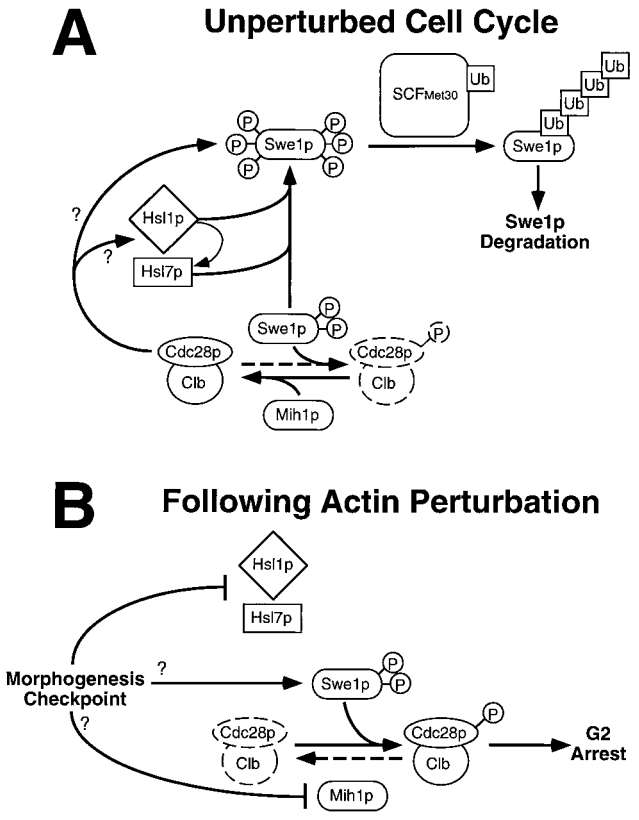

FIG. 8. Model for control of the *S. cerevisiae* cell cycle by the morphogenesis checkpoint. During the unperturbed cell cycle (A), Hsl1p and Hsl7p promote Swe1p hyperphosphorylation (P) leading to recognition by SCF^{Met30}, which catalyzes polyubiquitination (Ub), resulting in the subsequent degradation of Swe1p. Clb-Cdc28p complexes also contribute to Swe1p degradation, acting either through Hsl1p-Hsl7p or separately on Swe1p. Although Hsl7p can bind to Swe1p in the absence of Hsl1p, the fate of the complex may be regulated by Hsl1p-mediated phosphorylation of Hsl7p. The net effect of these interactions is to promote Swe1p degradation in G_2/M phase, which promotes the activation of Clb-Cdc28p complexes and hence the unimpeded progression of cells through mitosis. (Note, however, that the activity of Mih1p appears normally to be high enough to keep Clb-Cdc28p largely in the active state even if Swe1p degradation does not occur on schedule.) Following perturbation of the actin cytoskeleton (B), the morphogenesis checkpoint inhibits Hsl1p-Hsl7p, thus preventing Swe1p degradation. However, Swe1p stabilization alone is insufficient to promote G_2 arrest, and other checkpoint-responsive pathways must also act to regulate Swe1p and/or Mih1p, so that the balance of their activities is tilted in favor of the phosphorylation and inhibition of Cdc28p, leading to G_2 arrest.

not yet known whether Hsl1p can phosphorylate Swe1p directly and/or inhibit Swe1p kinase activity. Similarly, it is not known whether Nim1 influences Wee1 degradation in *S. pombe*, and it is possible that the phosphorylation of Swe1p by Hsl1p and of Wee1 by Nim1 functions both to inhibit their kinase activity and to target them for degradation. However, it is also possible that Hsl1p phosphorylates other substrates that are important for Swe1p degradation. One candidate is Hsl7p, which is in constant abundance through the cell cycle but is phosphorylated in an Hsl1p- and cell cycle-dependent manner; the cell cycle dependence may reflect the periodic accumulation of Hsl1p.

In addition to Hsl1p, there are two other Nim1-related kinases in *S. cerevisiae*, Gin4p and Ycl024Wp/Kcc4p (2, 4, 17, 25, 29, 39, 54). All of these kinases have diverged from Nim1 to similar extents (4, 17, 25), suggesting that they might play a redundant role in the down-regulation of Swe1p. However, Hsl7p phosphorylation did not occur, and Swe1p was completely stabilized in *hsl1*Δ mutants even though Gin4p and Kcc4p were present. These data suggest that Hsl1p (together with Hsl7p) plays a unique role in Swe1p regulation that is not shared with Gin4p or Kcc4p. The hypothesis that the Nim1-related kinases play distinct roles in *S. cerevisiae* is supported by the finding that Gin4p, but not Hsl1p or Kcc4p, is important for proper septin organization (25, 27).

Hsl7p is also important for targeting Swe1p for degradation. Hsl7p is a member of a protein family that is highly conserved across species but has no known biochemical activity or informative sequence motifs. Coimmunoprecipitation experiments indicate that Hsl7p is physically associated with Swe1p and that this association does not require the phosphorylation of Hsl7p or the presence of Hsl1p. Furthermore, the Hsl7p-Swe1p association also occurs in G_1-arrested cells, in which Swe1p is not hyperphosphorylated (48). These data suggest that the Swe1p-Hsl7p interaction might be a very early step in the targeting of Swe1p for degradation, preceding the accumulation of Hsl1p, the phosphorylation of Hsl7p, and the hyperphosphorylation of Swe1p (Fig. 8A).

In contrast to the apparent role of Hsl7p as a negative regulator of Swe1p, a recent study with *S. pombe* failed to identify a role for the Hsl7p homolog, Skb1, in regulating Wee1 (15). Instead, genetic interactions between *skb1*, *wee1*, and *cdc25* mutations suggested that Skb1, like Wee1, acts to delay entry into mitosis (15). It is not clear how to reconcile the seemingly opposite roles suggested for Hsl7p and Skb1, but it seems possible that the genetic interactions observed in *S. pombe* reflect an effect of *skb1* mutations in perturbing morphogenesis (or other processes) rather than a direct effect of Skb1 in cell cycle control.

Hsl1p, Hsl7p, and the morphogenesis checkpoint. Although Hsl1p and Hsl7p down-regulate Swe1p in unperturbed cells, *hsl1*Δ and *hsl7*Δ mutations appear to have no effect on Swe1p function in *cdc24* mutant cells undergoing a checkpoint response. This suggests either that Hsl1p and/or Hsl7p is itself down-regulated under checkpoint-inducing conditions (the model we prefer [Fig. 8B]) or that Swe1p is somehow protected from the action of Hsl1p and Hsl7p under these conditions.

We and others have shown that Hsl1p and Hsl7p, together with a fraction of cellular Swe1p, are localized to the mother-bud neck in a septin-dependent manner (4, 27, 36, 47). In addition, Barral et al. (4) made the intriguing observation that Hsl1p kinase activity (assayed by autophosphorylation in vitro) declined in septin mutants, suggesting that Hsl1p activity is dependent upon its proper localization. Because *cdc24* mutants fail to assemble a septin ring (20, 41), this suggests that Hsl1p would be inactive in these mutants, thus providing a mechanism for the proposed down-regulation of Hsl1p-Hsl7p by the morphogenesis checkpoint.

However, the model that the morphogenesis checkpoint-induced G_2 delay is due simply to Hsl1p delocalization in response to septin defects (4) is inconsistent with much of the available data. First, the checkpoint override observed in a *cdc24* mutant upon overexpression of Hsl1p or Hsl7p indicates that these proteins are able to function in the absence of assembled septins or neck structures, at least when present in excess. Second, Swe1p-dependent G_2 delays are triggered by several conditions (e.g., osmotic shock or treatment with latrunculin A in wild-type cells; *tpm1*Δ mutations) that affect the actin cytoskeleton but do not appear to affect septin organization or the mother-bud neck (33). Indeed, treatment with latrunculin A did not displace Hsl1p or Hsl7p from the neck (27). These conditions all cause Swe1p stabilization (48), suggesting that Hsl1p and Hsl7p are no longer effective in target-

ing Swe1p for degradation. It seems possible that the ability of Hsl1p and Hsl7p to down-regulate Swe1p can itself be down-regulated by more than one mechanism, but further research will be needed to test this hypothesis and to elucidate the pathway(s) involved.

Whatever the detailed mechanism(s) responsible for the checkpoint-induced stabilization of Swe1p, the data presented here also demonstrate that relieving the down-regulation of Swe1p by Hsl1p and Hsl7p is not sufficient to explain the checkpoint-induced G_2 delay. In our strain background, the deletion of *HSL1* or *HSL7* did not induce a detectable G_2 delay in otherwise wild-type cells during exponential growth, indicating that the G_2 delay caused by the morphogenesis checkpoint must involve additional pathways. Such pathways could include an increase in Swe1p specific activity, a change in Swe1p localization, or an inhibition of Mih1p, the phosphatase that counteracts Swe1p-mediated phosphorylation of Cdc28p (Fig. 8B). The last mechanism certainly has the potential to combine very effectively with Hsl1p-Hsl7p down-regulation, as *hsl1*Δ *mih1*Δ and *hsl7*Δ *mih1*Δ cells undergo a lethal Swe1p-dependent G_2 arrest.

Conclusions. We report here that Hsl1p and Hsl7p play a direct role in targeting Swe1p for degradation, and we suggest that down-regulation of the Hsl1p-Hsl7p pathway plays a role in the morphogenesis checkpoint response. Homologs of Hsl1p and Hsl7p have been identified in many species (8, 15, 21, 29). In *S. cerevisiae*, the control of Swe1p degradation is linked to the morphogenesis checkpoint. However, Wee1 degradation in *Xenopus* is regulated by the DNA replication checkpoint (34). It may be that a conserved degradation control pathway has been linked to different checkpoint sensors in different cells.

ACKNOWLEDGMENTS

We thank Y. Barral, D. Kellogg, A. Myers, M. Snyder, and J. Thorner for communicating results prior to publication. We thank Sally Kornbluth, Robin Wharton, John York, and Jake Harrison for critical reading of the manuscript, and the members of the Lew and Pringle labs for stimulating interactions.

J.N.M. and M.S.L. were supported by NIH postdoctoral fellowships GM18455 and GM15766, respectively. This work was supported by NIH grant GM31006 to J.R.P. and by NIH grant GM53050 and funds from the Searle Scholars Program/The Chicago Community Trust to D.J.L.

REFERENCES

1. **Adams, A. E. M., and J. R. Pringle.** 1984. Relationship of actin and tubulin distribution to bud growth in wild-type and morphogenetic-mutant *Saccharomyces cerevisiae*. J. Cell Biol. **98:**934–945.
2. **Altman, R., and D. Kellogg.** 1997. Control of mitotic events by Nap1 and the Gin4 kinase. J. Cell Biol. **138:**119–130.
3. **Bai, C., P. Sen, K. Hofmann, L. Ma, M. Goebl, J. W. Harper, and S. J. Elledge.** 1996. *SKP1* connects cell cycle regulators to the ubiquitin proteolysis machinery through a novel motif, the F-box. Cell **86:**263–274.
4. **Barral, Y., M. Parra, S. Bidlingmaier, and M. Snyder.** 1999. Nim1-related kinases coordinate cell cycle progression with the organization of the peripheral cytoskeleton in yeast. Genes Dev. **13:**176–187.
5. **Baudin, A., O. Ozier-Kalogeropoulos, A. Denouel, F. Lacroute, and C. Cullin.** 1993. A simple and efficient method for direct gene deletion in *Saccharomyces cerevisiae*. Nucleic Acids Res. **21:**3329–3330.
6. **Bi, E., and J. R. Pringle.** 1996. *ZDS1* and *ZDS2*, genes whose products may regulate Cdc42p in *Saccharomyces cerevisiae*. Mol. Cell. Biol. **16:**5264–5275.
7. **Booher, R. N., R. J. Deshaies, and M. W. Kirschner.** 1993. Properties of *Saccharomyces cerevisiae* wee1 and its differential regulation of $p34^{CDC28}$ in response to G_1 and G_2 cyclins. EMBO J. **12:**3417–3426.
8. **Chervitz, S. A., L. Aravind, G. Sherlock, C. A. Ball, E. V. Koonin, S. S. Dwight, M. A. Harris, K. Dolinski, S. Mohr, T. Smith, S. Weng, J. M. Cherry, and D. Botstein.** 1998. Comparison of the complete protein sets of worm and yeast: orthology and divergence. Science **282:**2022–2028.
9. **Coleman, T. R., Z. Tang, and W. G. Dunphy.** 1993. Negative regulation of the wee1 protein kinase by direct action of the nim1/cdr1 mitotic inducer. Cell **72:**919–929.
10. **Dunphy, W. G.** 1994. The decision to enter mitosis. Trends Cell Biol. **4:**202–207.
11. **Edgington, N. P., M. J. Blacketer, T. A. Bierwagen, and A. M. Myers.** 1999. Control of *Saccharomyces cerevisiae* filamentous growth by cyclin-dependent kinase Cdc28. Mol. Cell. Biol. **19:**1369–1380.
12. **Feldman, R. M., C. C. Correll, K. B. Kaplan, and R. J. Deshaies.** 1997. A complex of Cdc4p, Skp1p, and Cdc53p/cullin catalyzes ubiquitination of the phosphorylated CDK inhibitor Sic1p. Cell **91:**221–230.
13. **Ghiara, J. B., H. E. Richardson, K. Sugimoto, M. Henze, D. J. Lew, C. Wittenberg, and S. I. Reed.** 1991. A cyclin B homolog in *S. cerevisiae*: chronic activation of the Cdc28 protein kinase by cyclin prevents exit from mitosis. Cell **65:**163–174.
14. **Gietz, R. D., and A. Sugino.** 1988. New yeast-*Escherichia coli* shuttle vectors constructed with in vitro mutagenized yeast genes lacking six base pair restriction sites. Gene **74:**527–534.
15. **Gilbreth, M., P. Yang, G. Bartholomeusz, R. A. Pimental, S. Kansra, R. Gadiraju, and S. Marcus.** 1998. Negative regulation of mitosis in fission yeast by the shk1 interacting protein skb1 and its human homolog, Skb1Hs. Proc. Natl. Acad. Sci. USA **95:**14781–14786.
16. **Gilbreth, M., P. Yang, D. Wang, J. Frost, A. Polverino, M. H. Cobb, and S. Marcus.** 1996. The highly conserved *skb1* gene encodes a protein that interacts with Shk1, a fission yeast Ste20/PAK homolog. Proc. Natl. Acad. Sci. USA **93:**13802–13807.
17. **Hunter, T., and G. D. Plowman.** 1997. The protein kinases of budding yeast: six score and more. Trends Biochem. Sci. **22:**18–22.
18. **Jacobs, C. W., A. E. M. Adams, P. J. Szaniszlo, and J. R. Pringle.** 1988. Functions of microtubules in the *Saccharomyces cerevisiae* cell cycle. J. Cell Biol. **107:**1409–1426.
19. **Kaiser, P., R. A. L. Sia, E. G. S. Bardes, D. J. Lew, and S. I. Reed.** 1998. Cdc34 and the F-box protein Met30 are required for degradation of the Cdk-inhibitory kinase Swe1. Genes Dev. **12:**2587–2597.
20. **Kim, H. B., B. K. Haarer, and J. R. Pringle.** Unpublished results.
21. **Krapivinsky, G., W. Pu, K. Wickman, L. Krapivinsky, and D. E. Clapham.** 1998. pICln binds to a mammalian homolog of a yeast protein involved in regulation of cell morphology. J. Biol. Chem. **273:**10811–10814.
22. **Lew, D. J., and S. I. Reed.** 1995. A cell cycle checkpoint monitors cell morphogenesis in budding yeast. J. Cell Biol. **129:**739–749.
23. **Lew, D. J., and S. I. Reed.** 1993. Morphogenesis in the yeast cell cycle: regulation by Cdc28 and cyclins. J. Cell Biol. **120:**1305–1320.
24. **Lim, H. H., P.-Y. Goh, and U. Surana.** 1996. Spindle pole body separation in *Saccharomyces cerevisiae* requires dephosphorylation of the tyrosine 19 residue of Cdc28. Mol. Cell. Biol. **16:**6385–6397.
25. **Longtine, M. S., H. Fares, and J. R. Pringle.** 1998. Role of the yeast Gin4p protein kinase in septin assembly and the relationship between septin assembly and septin function. J. Cell Biol. **143:**719–736.
26. **Longtine, M. S., A. McKenzie III, D. J. DeMarini, N. G. Shah, A. Wach, A. Brachat, P. Philippsen, and J. R. Pringle.** 1998. Additional modules for versatile and economical PCR-based gene deletion and modification in *Saccharomyces cerevisiae*. Yeast **14:**953–961.
27. **Longtine, M. S., C. L. Theesfeld, J. N. McMillan, E. Weaver, J. R. Pringle, and D. J. Lew.** Unpublished data.
28. **Lorenz, M. C., R. S. Muir, E. Lim, J. McElver, S. C. Weber, and J. Heitman.** 1995. Gene disruption with PCR products in *Saccharomyces cerevisiae*. Gene **158:**113–117.
29. **Ma, X.-J., Q. Lu, and M. Grunstein.** 1996. A search for proteins that interact genetically with histone H3 and H4 amino termini uncovers novel regulators of the Swe1 kinase in *Saccharomyces cerevisiae*. Genes Dev. **10:**1327–1340.
30. **Maniatis, T., E. F. Fritsch, and J. Sambrook.** 1982. Molecular cloning: a laboratory manual. Cold Spring Harbor Laboratory, Cold Spring Harbor, N.Y.
31. **Mathias, N., S. L. Johnson, M. Winey, A. E. M. Adams, L. Goetsch, J. R. Pringle, B. Byers, and M. G. Goebl.** 1996. Cdc53p acts in concert with Cdc4p and Cdc34p to control the G_1-to-S-phase transition and identifies a conserved family of proteins. Mol. Cell. Biol. **16:**6634–6643.
32. **McMillan, J. N.** Personal communication.
33. **McMillan, J. N., R. A. L. Sia, and D. J. Lew.** 1998. A morphogenesis checkpoint monitors the actin cytoskeleton in yeast. J. Cell Biol. **142:**1487–1499.
34. **Michael, W. M., and J. Newport.** 1998. Coupling of mitosis to the completion of S phase through Cdc34-mediated degradation of Wee1. Science **282:**1886–1889. (Erratum, **283:**35, 1999.)
35. **Morgan, D. O.** 1997. Cyclin-dependent kinases: engines, clocks, and microprocessors. Annu. Rev. Cell Dev. Biol. **13:**261–291.
36. **Myers, A.** 1999. Personal communication.
37. **Nurse, P.** 1990. Universal control mechanism regulating onset of M-phase. Nature **344:**503–508.
38. **Ohi, R., and K. L. Gould.** 1999. Regulating the onset of mitosis. Curr. Opin. Cell Biol. **11:**267–273.
39. **Okuzaki, D., S. Tanaka, H. Kanazawa, and H. Nojima.** 1997. Gin4 of *S. cerevisiae* is a bud neck protein that interacts with the Cdc28 complex. Genes Cells **2:**753–770.
40. **Parker, L. L., S. A. Walter, P. G. Young, and H. Piwnica-Worms.** 1993.

Phosphorylation and inactivation of the mitotic inhibitor Wee1 by the nim1/cdr1 kinase. Nature **363:**736–738.

41. **Pringle, J. R., E. Bi, H. A. Harkins, J. E. Zahner, C. De Virgilio, J. Chant, K. Corrado, and H. Fares.** 1995. Establishment of cell polarity in yeast. Cold Spring Harbor Symp. Quant. Biol. **60:**729–744.
42. **Rhind, N., and P. Russell.** 1998. Mitotic DNA damage and replication checkpoints in yeast. Curr. Opin. Cell Biol. **10:**749–758.
43. **Richardson, H. E., C. Wittenberg, F. R. Cross, and S. I. Reed.** 1989. An essential G_1 function for cyclin-like proteins in yeast. Cell **59:**1127–1133.
44. **Rose, M. D., P. Novick, J. H. Thomas, D. Botstein, and G. R. Fink.** 1987. A *Saccharomyces cerevisiae* genomic plasmid bank based on a centromere-containing shuttle vector. Gene **60:**237–243.
45. **Russell, P., S. Moreno, and S. I. Reed.** 1989. Conservation of mitotic controls in fission and budding yeast. Cell **57:**295–303.
46. **Sherman, F., G. Fink, and J. B. Hicks.** 1982. Methods in yeast genetics. Cold Spring Harbor Laboratory, Cold Spring Harbor, N.Y.
47. **Shulewitz, M. J., C. J. Inouye, and J. Thorner.** 1999. Hsl7 localizes to a septin ring and serves as an adapter in a regulatory pathway that relieves tyrosine phosphorylation of Cdc28 protein kinase in *Saccharomyces cerevisiae*. Mol. Cell. Biol. **19:**7123–7137.
48. **Sia, R. A. L., E. S. G. Bardes, and D. J. Lew.** 1998. Control of Swe1p degradation by the morphogenesis checkpoint. EMBO J. **17:**6678–6688.
49. **Sia, R. A. L., H. A. Herald, and D. J. Lew.** 1996. Cdc28 tyrosine phosphorylation and the morphogenesis checkpoint in budding yeast. Mol. Biol. Cell **7:**1657–1666.
50. **Sikorski, R. S., and P. Hieter.** 1989. A system of shuttle vectors and yeast host strains designed for efficient manipulation of DNA in *Saccharomyces cerevisiae*. Genetics **122:**19–27.
51. **Skowyra, D., K. L. Craig, M. Tyers, S. J. Elledge, and J. W. Harper.** 1997. F-box proteins are receptors that recruit phosphorylated substrates to the SCF ubiquitin-ligase complex. Cell **91:**209–219.
52. **Sloat, B. F., A. E. M. Adams, and J. R. Pringle.** 1981. Roles of the *CDC24* gene product in cellular morphogenesis during the *Saccharomyces cerevisiae* cell cycle. J. Cell Biol. **89:**395–405.
53. **Stueland, C. S., D. J. Lew, M. J. Cismowski, and S. I. Reed.** 1993. Full activation of $p34^{CDC28}$ histone H1 kinase activity is unable to promote entry into mitosis in checkpoint-arrested cells of the yeast *Saccharomyces cerevisiae*. Mol. Cell. Biol. **13:**3744–3755.
54. **Tanaka, S., and H. Nojima.** 1996. Nik1: a Nim1-like protein kinase of *S. cerevisiae* interacts with the Cdc28 complex and regulates cell cycle progression. Genes Cells **1:**905–921.
55. **Wu, L., and P. Russell.** 1993. Nim1 kinase promotes mitosis by inactivating Wee1 tyrosine kinase. Nature **363:**738–741.